https://africanjournalofbiomedicalresearch.com/index.php/AJBR
Afr. J. Biomed. Res. Vol. 27 (September 2024); 543-559

Research Article

Therapeutic Potential Applications of Silver Nanoparticles Synthesized from *Cucurbita Maxima* for Wound Healing in Diabetic Male Albino Rats

Mona A. Yahya[1*], Fatma A. Al-Nefeiy[2], Ebtisam A. Bawazir[3]

[1*,2,3]*University of Jeddah, College of Science, Department of Biology, Jeddah, Saudi Arabia.*

Abstract

Objectives: A diabetic ulcer, or delayed wound recovery, is a significant complication of diabetes mellitus (DM), with its prevalence having risen steadily in recent decades. With the advancement of technology, nanoparticles have been used to treat wounds. Nanoparticles derived from pumpkin leaves (*Cm*AgNPs) are abundant in antioxidants and vitamins and possess antimicrobial and antiviral properties. This study highlighted the effectiveness of *Cm*AgNPs in accelerating wound healing.

Methods: Twenty-four male albino rats with partial-thickness wounds were assigned to four groups: the control group (NN), the untreated diabetes group (DN), the diabetic group treated with (*Cm*AgNPs), and the group treated with silver sulfadiazine (SSD) cream. Morphological, histopathological, and physiological assessments of inflammation were conducted on all rats at 0-, 7-, 14-, and 21-days post-treatment.

Results: On days 0, 7, 14, and 21, histological examination was conducted. Also, the activities of glutathione (GSH) and superoxide dismutase (SOD) were assessed. Histological analysis demonstrated that *Cm*AgNPs significantly increased collagen content in the wound tissue and facilitated re-epithelialization. On days 7, 14, and 21, the group treated with *Cm*AgNPs exhibited higher GSH levels compared to the DN and SSD groups. However, *Cm*AgNPs did not have a significant effect on SOD levels.

Conclusion: By stimulating re-epithelialization and collagen synthesis, (*Cucurbita maxima*) demonstrated superior efficacy in treating diabetic wound compared to silver sulfadiazine ointment.

Keywords: Diabetic ulcer, Wound healing, silver nanoparticles (CmAgNPs), Re-epithelialization, Collagen synthesis.

***Author for correspondence: Email:** myahya0008.stu@uj.edu.sa

Received; 08/07/2024 Accepted: 10/08/2024

DOI: https://doi.org/10.53555/AJBR.v27i3.1760

Introduction

Tissue injuries, including wounds, can result from physical, chemical, or mechanical trauma. Bacterial infections are prevalent, which impede the process of healing by causing inflammation and tissue injury. Critical to the health of all patients, including diabetics, is the issue of wound healing [1].

Diabetes mellitus (DM) is a highly debilitating chronic metabolic disorder, marked by significant physiological changes in both cells and tissues [2]. Various factors contribute to the delayed recovery of wounds, including oxidative stress, re-epithelialization, keratinocyte, fibroblast migration, proliferation and growth factor production and inflammatory response [3]. Significant characteristics of diabetic vascular complications include persistent inflammation and elevated oxidative stress. Enhanced oxidative stress hinders the process of wound healing in individuals with diabetes through its impact on a range of cytokines and growth factors [4].

Since most diabetic wound infections are resistant to medications, they may result in higher expenses, morbidity, and mortality [5]. Thus, an ongoing endeavor is to identify cost-effective agents without adverse effects capable of expediting the healing process of diabetic lesions. Utilizing natural products in conjunction with nanotechnology to promote the expeditious healing of wounds [6,7].

Pumpkin (*Cucurbita maxima Duchesne*) is a member of the *Cucurbitaceae* family. *Cucurbita maxima* is a plant extensively cultivated in most temperate regions of the globe, including India, for both medicinal and vegetable purposes. Additionally, vitamins and amino acids are abundant in the leaves as antidiabetic, anti-inflammatory, immuno-modulatory, and antibacterial agents for wound healing [8].

In vitro studies have demonstrated that silver sulfadiazine (SSD), a prevalent anti-infective agent utilized to inhibit bacterial proliferation and hypothesized to be efficacious in diminishing the inflammatory and granulation phases of the healing process, is cytotoxic to keratinocytes and fibroblasts. It is the topical agent most commonly used to treat wounds [9].

Methodology

Preparation of aqueous extract of Pumpkin leaves:

1 gram of finely powdered pumpkin leaves was dissolved in 100 mL of distilled water and heated for 30 minutes at a temperature of 60-70°C. The resulting extract was filtered using Whatman No. 1 filter paper and subsequently used in biosynthesis experiments for nanoparticle production [10].

Biosynthesis of AgNPs using plants (Pumpkin leaves) aqueous extracts:

The environmentally friendly production of silver nanoparticles (*Cm*AgNPs) was completed using the method outlined by [11] with little modification. 1 mM silver nitrate ($AgNO_3$) was added to plants extract to promote the formation of *Cm*AgNPs. The plants extract (1, 2, 3, 4 and 5 mL) were added drop by drop each time to 10 mL of 1 mM silver nitrate solution with constant stirring for 60 min at 60-70 °C and incubated in a dark bottle to minimize photo-activation of silver nitrate. The pH value of resulting solution was measured to be about 7.0. The color of the solution was changed to dark brown gradually with increasing time of mixing. After 60 min the complete reaction was performed indicating the complete reduction of Ag^+ to Ag^0 which was further confirmed by using UV-Visible spectroscopy. The silver nanoparticles obtained by plants extract were centrifuged at 15,000 rpm for 10 min and then dispersed in sterile distilled water and sonicated in a sonication water bath for 15 min at 65 °C to get rid of any clumsy materials.

Experimental Animal

This study was approved by the Research Ethics Committee of King Abdulaziz University, under the MSF ethical reference number (Ref: p101-2022). Twenty-four male Albino rats, ranging in weight from 150 to 250, were utilized in this research. With a 12-hour light-dark cycle, each rat was maintained at a controlled temperature of 22 ± 1°C. Ample water was provided to them in addition to standard laboratory food. Preceding the experiment by three days, each animal was individually acclimated in a separate cage.

STZ (Wako Chemical Co., Osaka, Japan), a toxin that specifically targets the cells that produce insulin, was administered intravenously at a rate of 65 mg/kg in a saline-sodium citrate buffer (pH 4.5; Sigma, Inc., St. Louis, MO), to induce diabetes in all experimental groups (DN, SSD, and *Cm*AgNPs [12]. A swift glucometer (ACCU-CHECK Active® Germany) was employed to ascertain the blood glucose levels [13]. Animals were classified as diabetic and included in the study if their blood glucose levels exceeded 300 mg/dL one week following STZ injection [14].

Deep Partial-Thickness wound Induction.

For all of the experiments in this investigation, rats were anesthetized intraperitoneally with ketamine/xylazine (60 mg/kg ketamine and 10 mg/kg xylazine) [15]. On the day of surgery (day 0), the dorsal epidermis of the animal is shaved and disinfected with 70% ethanol. Additionally, a sterile medical scalpel was used to create a 1 cm diameter excision on the dorsal epidermis. Rats were confined to sanitized individual cages after their anesthesia recovery [16]. The wound degree was confirmed histopathologically using H&E staining.

Wound closure rate

Wound closure rate (WCR) was determined by taking consecutive photos of the wounds on days 0, 7, 14, and 21 after wounding with a digital camera (Coolpix 5400, Nikon, Japan) and a scale (as a reference). Using image analysis software (ImageJ Software, USA), the wound area was assessed. During the experiment, the initial and subsequent areas of the wound were utilized to compute the rate of wound closure using the formula below: [17] % wound closure = [(day 0 area - day (n) area)/day 0 area] X 100, where n is the number of days (0, 7, 14 and 21).

Wound treatment

For 21 days, each rat in the group treated with Silver Nanoparticles derived from pumpkin leaf extract (*Cm*AgNPs) received a topical application of a 1 mL dose. In the SSD group, wounds were simply covered with a daily layer of silver sulfadiazine cream (1/16 inch thick) for 21 days, following the manufacturer's instructions. No treatment was given to the wounds of the NN and DN groups. During the duration of the experiment, the wounds remained exposed.

Study Design

Twenty-four rats were categorized into four distinct categories, six comprising each group. The process of allocating rats to study groups was as follows: Group (1) functioned as the control group and did not receive any treatment. Group (2) comprised diabetic rats that did not receive any form of treatment. Group (3) consisted of diabetic rats with wounds that were topically treated with 1 mL of *Cm*AgNPs. The nanoparticles were applied directly to the wound site and allowed to remain for 5 minutes. Subsequently, a sterile plastic drape was applied to the wounds and surrounding tissues once daily. Lastly, Group (4) was administered silver sulfadiazine cream (Flamazine®) as the standard wound treatment. The study spanned 21 days, during which wound induction was designated as day 0, and treatment commenced on the following day, denoted as day 1. A total of two rats from each group were subjected to cervical dislocation as the method of euthanasia after the study period on days 0, 7, 14 and 21.

Morphological Analysis

Following previously established protocols [18,19], morphological alterations were evaluated concerning redness

color, edema, and wound bed dryness. Morphological changes in the skin wounds were documented by acquiring photographs on days 0, 7, 14, and 21 after the treatment. Every day, the same researcher observed and documented developments in the wounds.

Collection of blood samples

Blood specimens were obtained from the jugular vessels of fasted rats anesthetized with diethyl ether at 0, 7, 14, and 21 days of treatment. Before centrifuging the blood at 3000 rpm for 15 minutes, it was allowed to coagulate at room temperature. Three Eppendorf tubes were fractionated, and the supernatant sera were sucked.

Determination of oxidant/antioxidant system parameters

The activity of glutathione peroxidase (GSH) was evaluated by preparing tissue homogenates and applying a colorimetric assay reagent (Cat. No. 703102, Bayman Chemical, Michigan, USA) as described by [20]. Superoxide dismutase (SOD) levels in the tissue homogenates were measured using spectrophotometric techniques, following the method outlined by [21]. Malondialdehyde (MDA) concentrations were determined spectrophotometrically using the thiobarbituric acid method, summarized as per the protocol in [23].

Histopathological Evaluation of Inflammation

Histological examination of wound tissue was conducted on days 0, 7, 14, and 21 for all experimental groups to acquire high-quality sections suitable for microscopy. Another segment of cutaneous tissue was preserved for 24 hours in 10% formalin. Then, the fixed tissues were dehydrated in a gradual series of ethyl alcohol from 70%, 80%, 90%, 96%, and 100% for 2 h, respectively. The samples were cleared in xylene to remove aqueous fixative and tissue water. In conclusion, fixed skin samples from every group were embedded in paraffin, sectioned into 5µm thick sections and stained using hematoxylin and eosin (H&E) [24].

Statistical Analysis

The mean (M) was calculated for both the control and treated groups, along with the standard error (SE) for means. Analysis of variance (ANOVA) tests and t-tests were conducted at a 5% significant level. Additionally, the percentage of change compared to the control was determined [25,26].

Results

Characterization of Pumpkin-Derived Silver Nanoparticles (*Cm*AgNPs)

Following established protocols, the synthesized silver nanoparticles displayed a distinct surface plasmon resonance (SPR) peak at around 442.04 nm, confirming their successful formation. Transmission Electron Microscopy (TEM) analysis revealed spherical nanoparticles with an average diameter of 16.05 ± 0.02 nm. Fourier-transform infrared spectroscopy (FTIR) analysis revealed the presence of functional groups from the *Cucurbita maxima* extract, which are likely responsible for facilitating the biosynthesis and stabilization of nanoparticles. Comprehensive characterization details are available in the supplementary materials (**Fig. S1**).

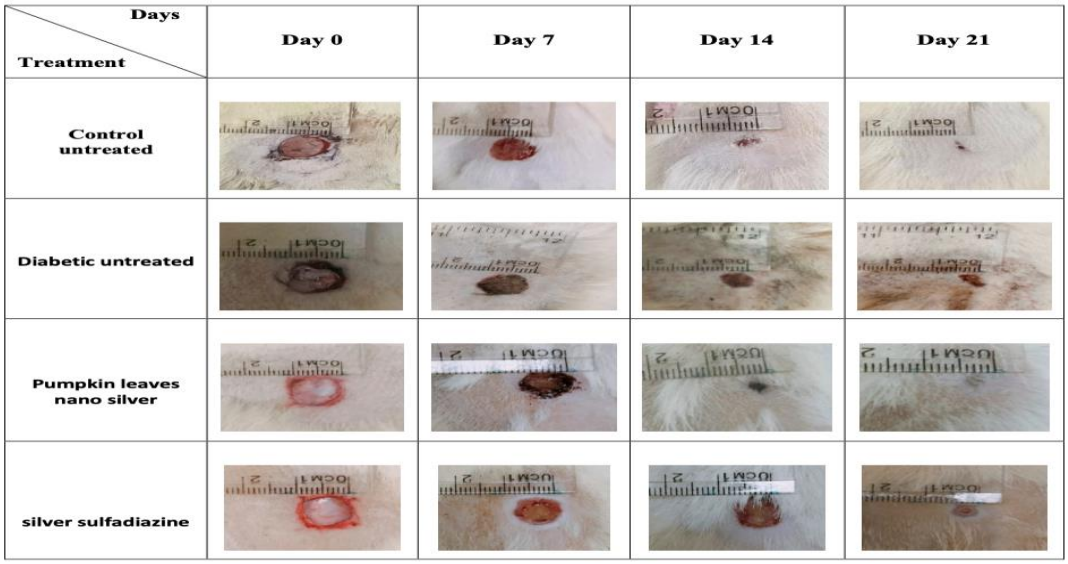

Fig. 1. Macroscopic images of wounds from all groups, illustrating the progression of wound closure on days 0, 7, 14, and 21. NN: non-diabetic untreated group; DN: diabetic untreated group; Pumpkin leaves nano silver-treated group; SSD: silver sulfadiazine cream-treated diabetic group.

Morphology studies

In both undiabetic and diabetic rats, in the SSD group and diabetic groups treated with pumpkin leaves nano silver, there was a gradual reduction and contraction of the wound area observed by day 7.

Furthermore, diabetic rats exhibited increased wound contraction at days 14 and 21 post-injury and slightly improved. In conclusion, rats from the diabetic groups treated with pumpkin leaves (*Cucurbita maxima*) nanoparticles (*Cm*AgNPs)

demonstrated the most significant healing among all groups (Fig. 1).

Wound closure rate.

WCR in the pumpkin leaf nanoparticles (*Cm*AgNPs) group was significantly (P<0.05) higher compared to both DN and SSD groups on day 14 and 21 as well as to NN group on day 7. SSD group showed significant (P<0.05) higher WCR on all days compared to DN group (Fig. 2).

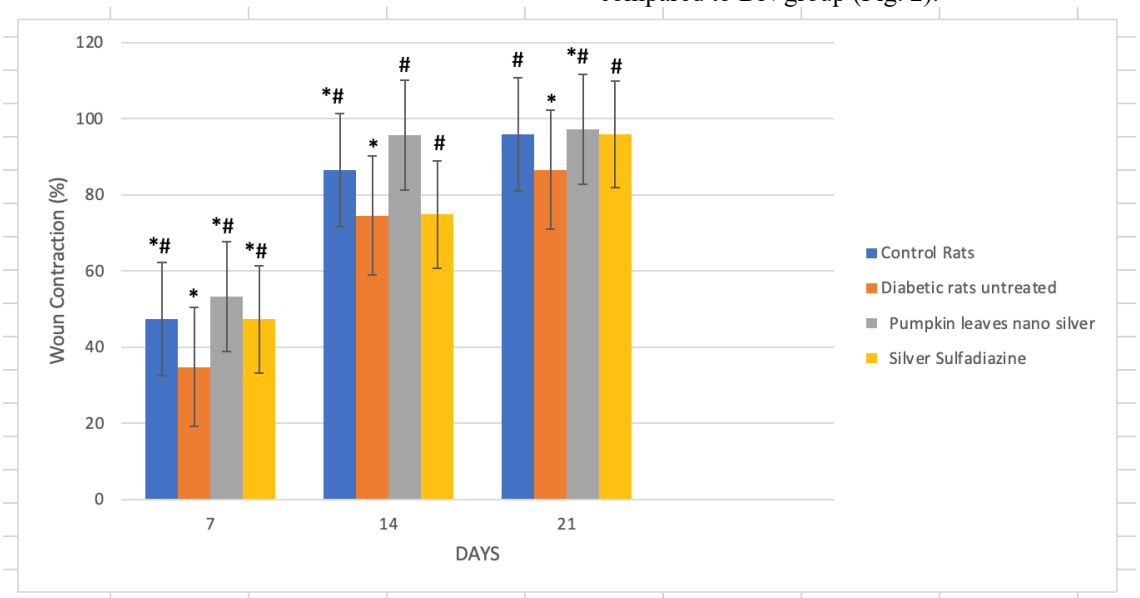

Fig. 2. Wound Closure Rate (WCR) of all groups on days 7, 14, and 21. The WCR of the pumpkin leaf nanoparticles group (*Cm*AgNPs) was significantly higher compared to the DN group on all days and to the SSD group on days 14 and 21 (P<0.05). *Indicates a significant difference compared to the SSD group (P<0.05). # Indicates a significant difference compared to the DN group (P<0.05).

Plasma glucose values

Diabetic and non-diabetic rats were enrolled in the experiment. Twenty-four rats were initially enlisted. As described in the Research Design and Method section, STZ induced diabetes in half of the rats.

The administration of treatments was conducted in the group of diabetic rats. Mean blood glucose levels for each group were measured on the initial day of treatment with *Cm*AgNPs and SSD. Moreover, these values were recorded on days 7, 14, and 21 of treatment (following injury) and immediately before their demise. The data are presented in (Fig. 3) Table (1).

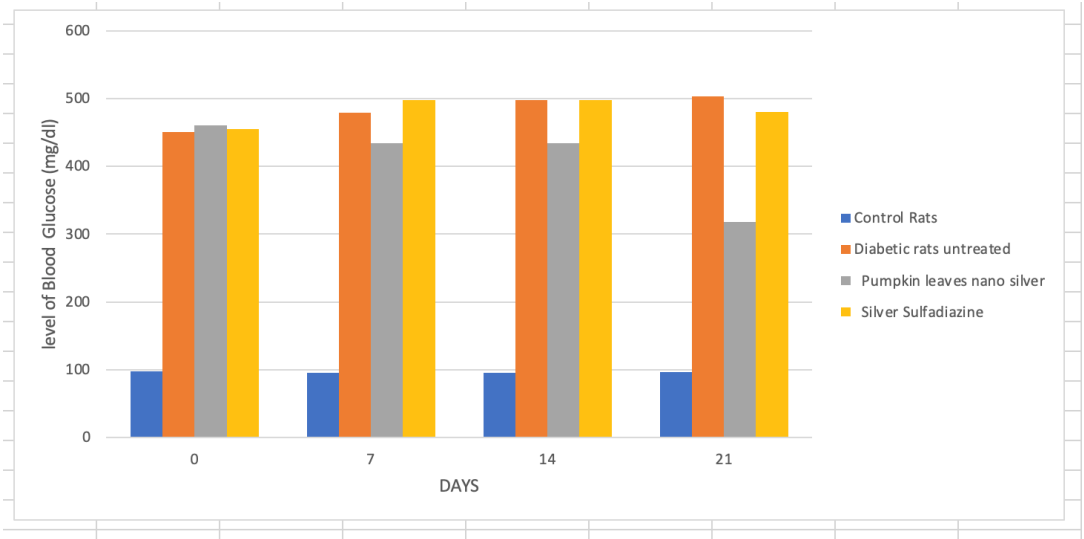

Fig. 3. The effect of Biogenic applications on wound healing was evaluated by measuring blood glucose levels (mg/dL) in normal and diabetic rats.

Table (1). Effect of Biogenic Nano Silver (*Cm*AgNPs) on Wound Healing by Measuring Blood Glucose Levels (mg/dL) in Normal and Diabetic Male Rats.

Treatment / No. of days	Control	Diabetic rats untreated	Pumpkin leaves nano silver	Silver Sulfadiazine
0	97 ± 6.03	450 ± 34.922	460 ± 66.683	455 ± 50.207
7th	95 ± 6.675	479 ± 42.224	433 ± 42.435	497 ± 39.865
14th	95 ± 6.675	497 ± 42.224	433 ± 42.435	497 ± 39.86
21st	96 ± 5.827	502 ± 44.122	318 ± 23.094	480 ± 34.930

Data means ± SD based on 6 rats per group.

SOD & GSH

(Fig. 4) showed the effect of Biogenic nano silver for Wound Healing on level of Superoxide dismutase (SOD) (µ/mL) of normal and diabetic in male rats.

Comparison between the level of SOD in deferent student groups with control group were showing in (Fig. 4) level of SOD was significantly decrease in all groups (at day 0), diabetic group (at day 7, 14, 21) and sulfadiazine group (at day 21). A significant increase in SOD levels was observed in the group treated with *Cm*AgNPs on days 7 and 14, as well as in the sulfadiazine-treated group on day 14. There was a significant increase in SOD levels were elevated at all measured intervals on days 7, 14, and 21 in both the *Cm*AgNPs-treated and sulfadiazine groups compared to the diabetic control rats. Notably, the SOD level was significantly higher in the *Cm*AgNPs group on day 21 compared to the silver sulfadiazine group.

(Fig. 5) showed the effect of Biogenic nano silver for Wound Healing on level of Glutathione (GSH) (µg/mg) of normal and diabetic in male rats.

A significant decrease in the level of GSH was recorded in day 0, 7, 14, 21 of all deference groups compared to control.

However, there was a significant increase in GSH levels on all days in both the *Cm*AgNPs-treated and silver sulfadiazine groups compared to the untreated diabetic group.

GSH levels were significantly higher in the *Cm*AgNPs-treated group on days 0 and 7 compared to the silver sulfadiazine group.

Diabetic groups showed significant decrease in the level of GSH in all intervals compared to control.

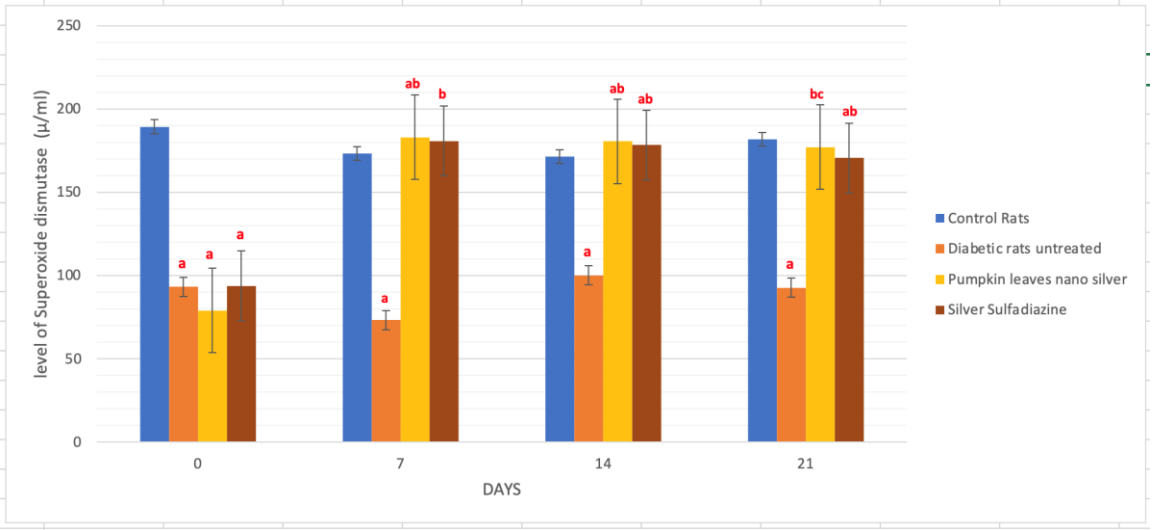

Fig. 4. The effect of Biogenic applications on wound healing was assessed by measuring Superoxide Dismutase (SOD) levels (µ/mL) in normal and diabetic rats. Statistical analyses were conducted on control (C=6) and treated (T=6) animals with the following comparisons: *a* statistically significant (*P*<0.05) compared to the normal control group, *b* statistically significant (*P*<0.05) compared to the diabetic group, *c* statistically significant (*P*<0.05) compared to the Silver Sulfadiazine group.

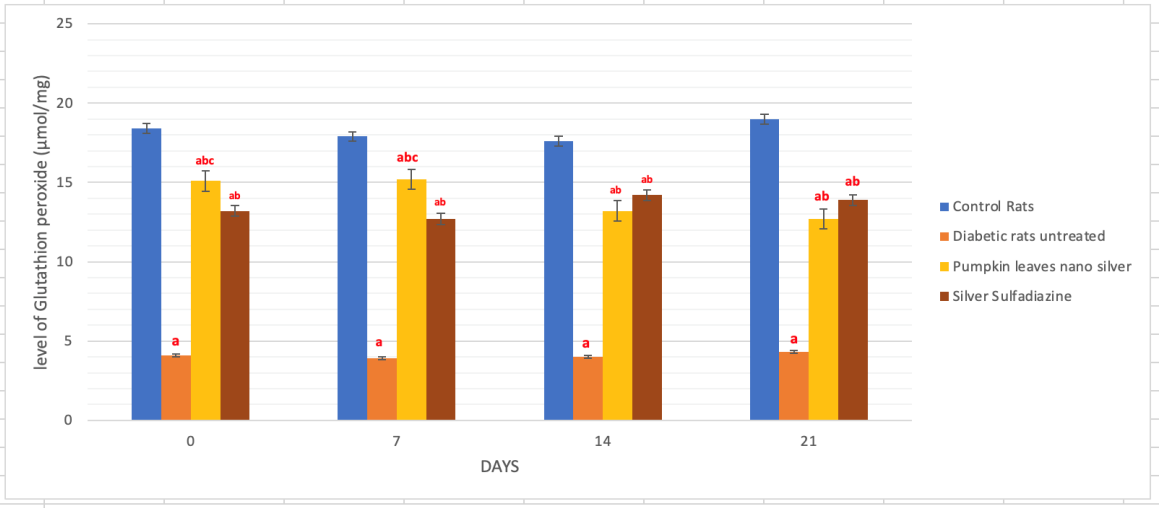

Fig. 5. The effect of Biogenic applications on wound healing was evaluated by measuring Glutathione (GSH) levels (µmol/mg) in normal and diabetic rats. Statistical analyses were performed on control (C=6) and treated (T=6) animals using the following comparisons: *a* statistically significant (*P*<0.05) compared to the normal control group, *b* statistically significant (*P*<0.05) compared to the diabetic group, *c* statistically significant (*P*<0.05) compared to the Silver Sulfadiazine group.

MDA.

(Fig. 6) showed the effect of Biogenic nano silver for Wound Healing on level of Malondialdehyde (MDA) (nmol/g) of normal and diabetic in male rats. A significant increase in the level of MDA was recorded in day 0, 7, 14, 21 of all deference groups compared to control group.

There was no significant difference in MDA levels among all groups on day 0. However, MDA levels significantly increased in both the *Cm*AgNPs-treated and silver sulfadiazine groups on days 7, 14, and 21 compared to the diabetic group.

On day 0, there were no significant differences in MDA levels among all groups. However, there was a significant decrease in MDA levels in the *Cm*AgNPs-treated group on day 21 compared to the silver sulfadiazine group.

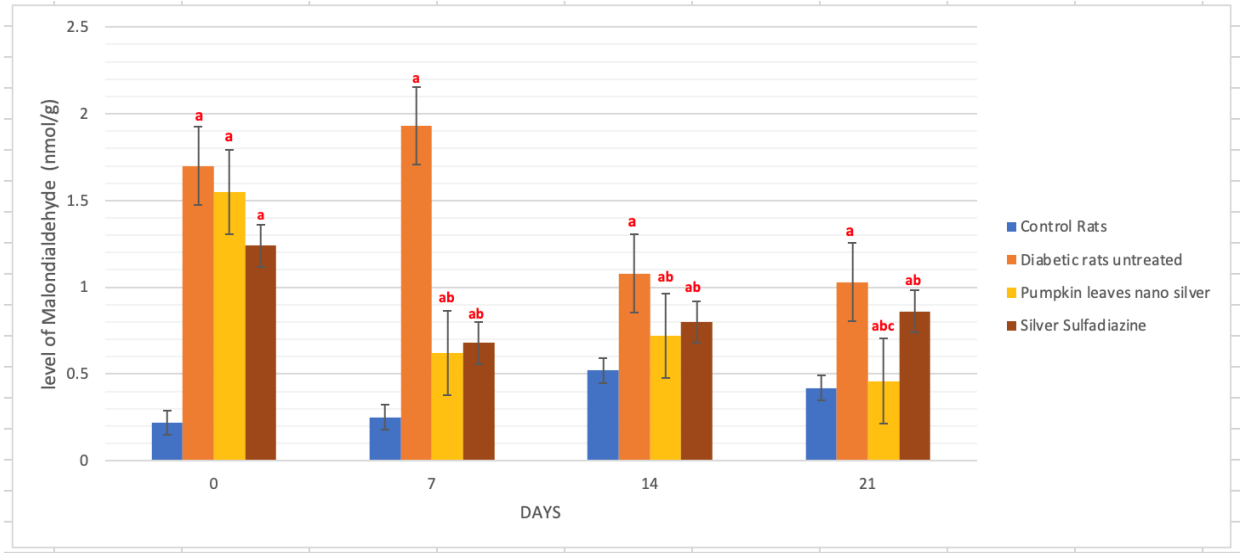

Fig. 6. The effect of Biogenic applications on wound healing was assessed by measuring Malondialdehyde (MDA) levels (nmol/g) in normal and diabetic rats. Statistical analyses were conducted on control (C=6) and treated (T=6) animals using the following comparisons: *a* statistically significant (*P*<0.05) compared to the normal control group, *b* statistically significant (*P*<0.05) compared to the diabetic group, *c* statistically significant (*P*<0.05) compared to the Silver Sulfadiazine group.

Histological analysis.

Rat skin typically comprises three distinct layers: the epidermis, dermis, and subcutis. The epidermis, which is in direct contact with the exterior, is a stratified squamous epithelium characterized by its high specialization and self-regeneration. Within this epithelium, keratin, a strong, protective protein, is

partially water-resistant. The epidermis is intricately connected to the dermis by a specialized basement membrane.

The dermis is a strong layer made up of fibroblasts and collagen and elastic fibers organized horizontally. The dermis adjacent to the epidermis is less dense and contain numerous small blood vessels. The subcutis, a layer of adipose tissue, is the third layer. In addition to storing fat, serves as a heat insulator and shock absorber.

Control Group:

On day 0, The control group revealed a lack of collagen production, inflammatory cell infiltration, coagulative necrosis of surface epithelium and dermal connective tissue, blood vessels, and adnexa.

On the 7th postoperative day, injuries confined No new collagen and very few new arteries were seen, and wounds contained a discrete epithelialization was noticed. There has been noticeable progress in terms of inflammatory cell infiltration.

On the 14th postoperative day, the Control group exhibited a dense extracellular matrix with thinner, more disorganized collagen fibers and moderate inflammatory infiltration. The dermis also contained numerous blood vessels, a granular layer, and a complete scar formation.

On the 21st postoperative day, the wounds of untreated rats were still not fully healed, with a reduced number of inflammatory cells present in the scar tissue. Upon re-epithelialization, the epidermis showed excessive thickening in the wound area. In the Control group, slight inflammatory infiltration was observed in the wounds, along with a reduction in the number of blood vessels (Fig. 7).

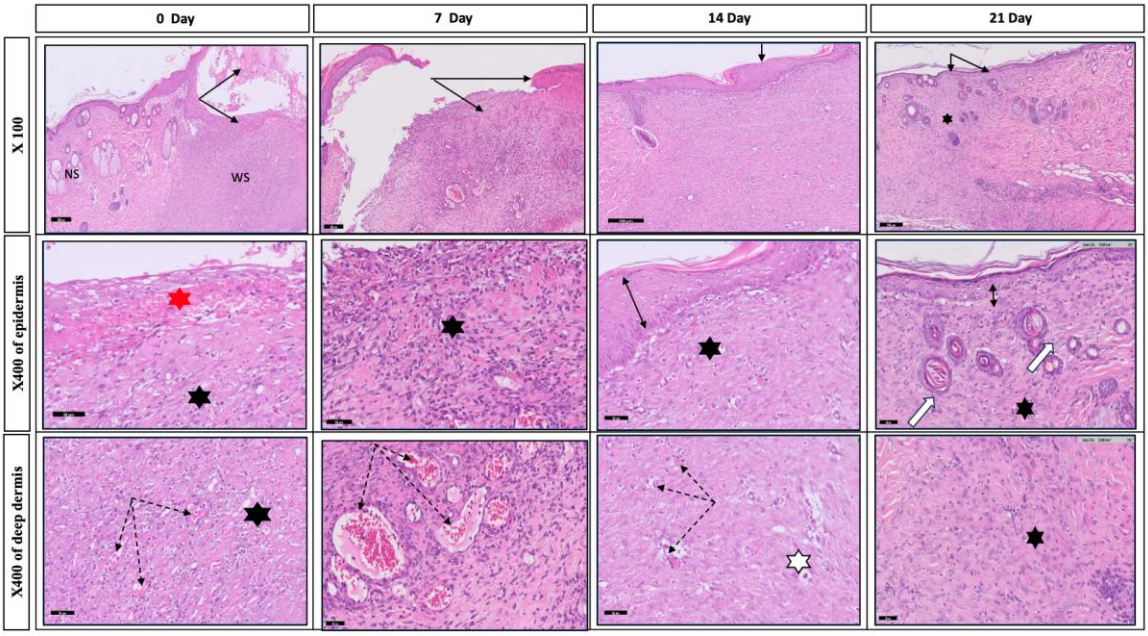

Fig. 7. Representative images of H&E-stained histological sections of wounds from the control group (untreated) rats on days 0, 7, 14, and 21 post-wounding (magnifications x100, x400). The images show normal skin (NS) and wound skin (WS), with a large scab (arrows) marked as wound scab (red star). Congested vessels are indicated by dotted arrows, and inflammatory cells are noted with a black star, highlighting the lack of collagen formation. Collagen is marked with a white star, and the double-headed arrow points to proliferating hyperplastic epidermis.

Diabetic Groups:

Seven days post-wounding, diabetic wounds that remained untreated exhibited insufficient collagen deposition. Histological changes in the epidermis included large scabs, infiltration of inflammatory cells, epithelial and dermal damage, and an increase in blood vessels. Compared to the control groups, the untreated diabetic wounds demonstrated delayed wound healing.

On Day 14 after wounding, untreated diabetic rats with wounds showed signs of scab accumulation, a thinner epidermis, and an increase in blood vessels and inflammatory cell infiltration in the dermis. It is evident that the regulatory tissue's attempt to compensate for the healing deficit occurs when collagen deposition is insufficient to create a mature matrix that will maintain the wound. After 14 days, re-epithelialization was seen; the diabetic non-treated group showed fewer cellular layers than the control group.

On Day 21 after wounding, nontreated diabetic rats showed collagen synthesis in their wounds and a postponement of the inflammatory phase. wound tissues of nontreated diabetic showed much slower healing than the treated diabetic rats, according to histological alterations (Fig. 8).

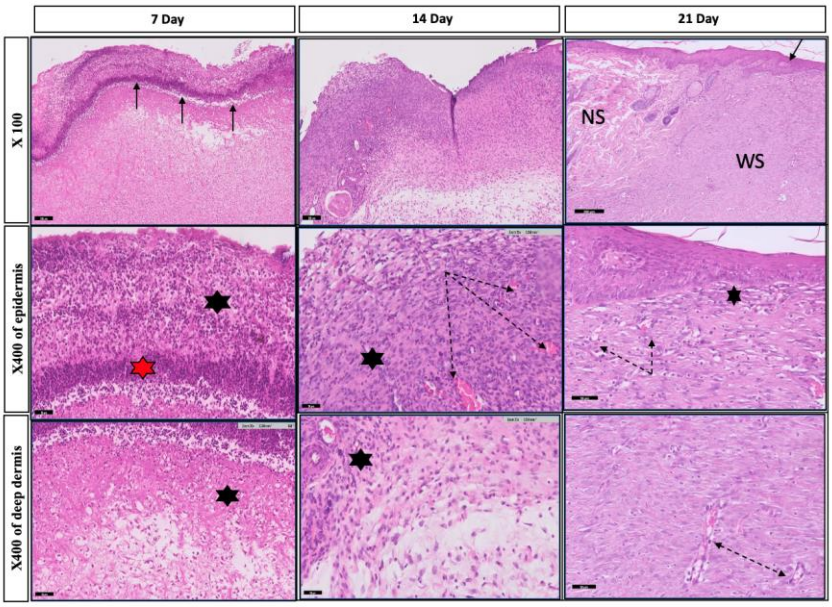

Fig. 8. Representative images of H&E-stained histological sections of wounds from the diabetes group (untreated) rats on days 7, 14, and 21 post-wounding (magnifications x100, x400). The images display normal skin (NS) and wound skin (WS) with disorganization of the wound surface and formation of a large scab (thin arrows), highlighted as wound scab (red star). Inflammatory cells with minimal collagen formation are marked (black star), along with congested vessels (dotted arrows). The wound skin also shows prominent features of re-epithelialization. (thin arrow).

Pumpkin leaf nanoparticles (*Cm*AgNPs):

On the 7th postoperative day, the *Cm*AgNPs-treated groups showed increased levels of collagen fibers, a large presence of inflammatory cells, and incomplete re-epithelialization.

On the 14th postoperative day, the group treated with leaf extract exhibited a thicker and more distinct epidermal layer compared to the dermis, which displayed a more organized structure. The dermis contained few blood vessels and a high number of proliferating fibroblasts. Some inflammatory cells were present, and the collagen fibers appeared thick and uniform.

On the 21st postoperative day, re-epithelialization was observed, with a slight reduction in skin tissue damage. The dermis displayed a high density of connective tissue collagen fibers, normal cells, and an increased number of fibroblasts, while the wrinkled epidermis showed extensive regeneration. The improved wound closure in this group may be attributed to the higher fibroblast count (Fig. 9).

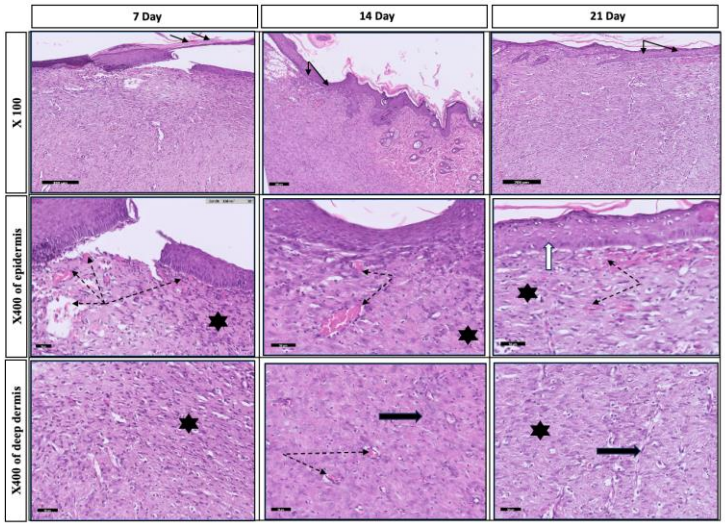

Fig. 9. Representative images of H&E-stained histological sections of wounds from the pumpkin leaf nanoparticles group (Cucurbita maxima treatment) rats on days 7, 14, and 21 post-wounding (magnifications x100, x400). The images show a large scab (thin arrows), inflammatory cells with minimal collagen formation (black star), and congested blood vessels (dotted arrows) with numerous proliferating fibroblasts. On day 14, the thin arrow indicates effective healing with no scab and signs of re-epithelialization. By day 21, the thick white arrow points to the wound surface with hyperplastic epithelialization, while the thick black arrows highlight normal epithelium, collagen, and fibroblasts.

Sulfasalazine Cream Group:

On the 7th postoperative day, the wound tissue showed a damaged epidermis, while wounds treated with SSD displayed higher levels of epithelialization, with increased cellular infiltration and lower collagen content. Neovascularization was also evident on day 7 in diabetic rats treated with Sulfadiazine.

By the 14th postoperative day, fibrosis in the dermis had extended to the subcutaneous tissue. By this time, the scab had fallen off in the SSD group, but the epidermis had not fully regenerated. Compared to the diabetic groups, the SSD group's epithelial layer appeared more favorable. Additionally, the wounds exhibited a moderate level of collagen, and the acute inflammatory response had diminished by day 14.

On the 21st postoperative day, the slow progression of silver sulfadiazine in re-epithelialization may have contributed to impaired wound healing at the early stages. By day 21, diabetic rats treated with sulfadiazine showed no signs of chronic inflammation. However, by the end of the experiment, the sulfadiazine group had achieved full re-epithelialization. Neovascularization was not observed on day 21 (Fig. 10).

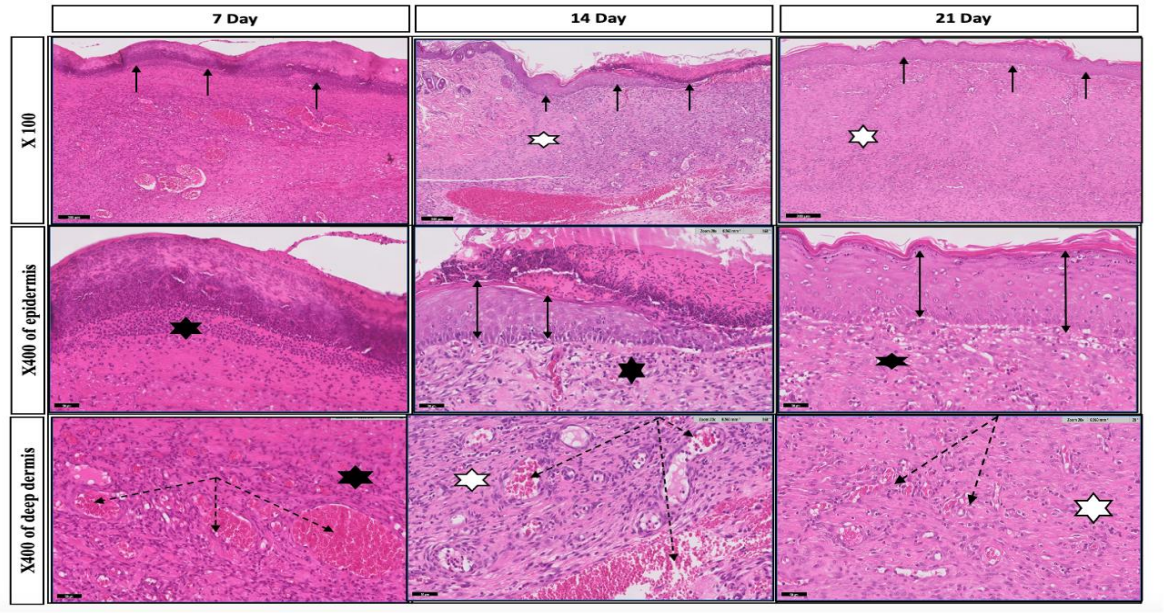

Fig. 10. Representative images of H&E-stained histological sections of wounds from the diabetes group treated with Silver Sulfadiazine on days 7, 14, and 21 post-wounding (magnifications x100, x400). The wound skin displays disorganization of the surface wounded area with the formation of a large scab (thin arrows), inflammatory cells (black star), and congested blood vessels (dotted arrows). On day 14, the wound surface shows hyperplastic epithelialization (thin arrows), collagen (white star), and proliferating hyperplastic epidermis (double-headed arrow).

Analysis of histology by Masson's Trichrome stain the pumpkin leaf nanoparticles (*Cm*AgNPs) group and the NN group showed intact epidermis with formed dermal papillae when their wound tissue was stained with trichrome, but the DN and SSD groups showed damaged epidermis.

On day 7 it was revealed that the NN groups and pumpkin leaf nanoparticles (*Cm*AgNPs) had a high collagen content. Conversely, there was increased cellular infiltration and decreased collagen levels in the DN and SSD groups.

On day 14, all groups showed complete epithelialization. In contrast, the *Cm*AgNPs group displayed a completely developed epidermis with effective dermal epidermal interdigitation. *Cm*AgNPs and the NN groups demonstrated more collagen fibers arranged in an extremely well-organized fashion coupled with fibroblasts that mimicked normal skin. The DN and SSD groups, on the other hand, displayed a modest level of collagen.

On day 21, the appearance of blue-colored stains in the light microscopy pictures of the scar tissues revealed a good degree of collagen deposition in the groups treated with pumpkin leaf nanoparticles (*Cm*AgNPs). Additionally, the skin structure appeared to have nearly fully returned to its pre-wound form. Surprisingly, SSD and the untreated groups had far less collagen deposition (Table 2.) (Fig. 11, 12, 13, 14).

Table (2). Effects of Therapeutic Applications on Collagen Scores Across Different Groups.

Treatment / No. of days	Control rats untreated	Diabetic rats untreated	Pumpkin leaves nano silver	Silver Sulfadiazine
0	-	-	-	-
7th	+	-	++	+
14th	++	+	+++	++
21st	++	+	++++	+++

Note: Collagen was evaluated using Masson trichrome staining and scored as negative (–), mild (+), mild to moderate (++), moderate (+++), and intense (++++).

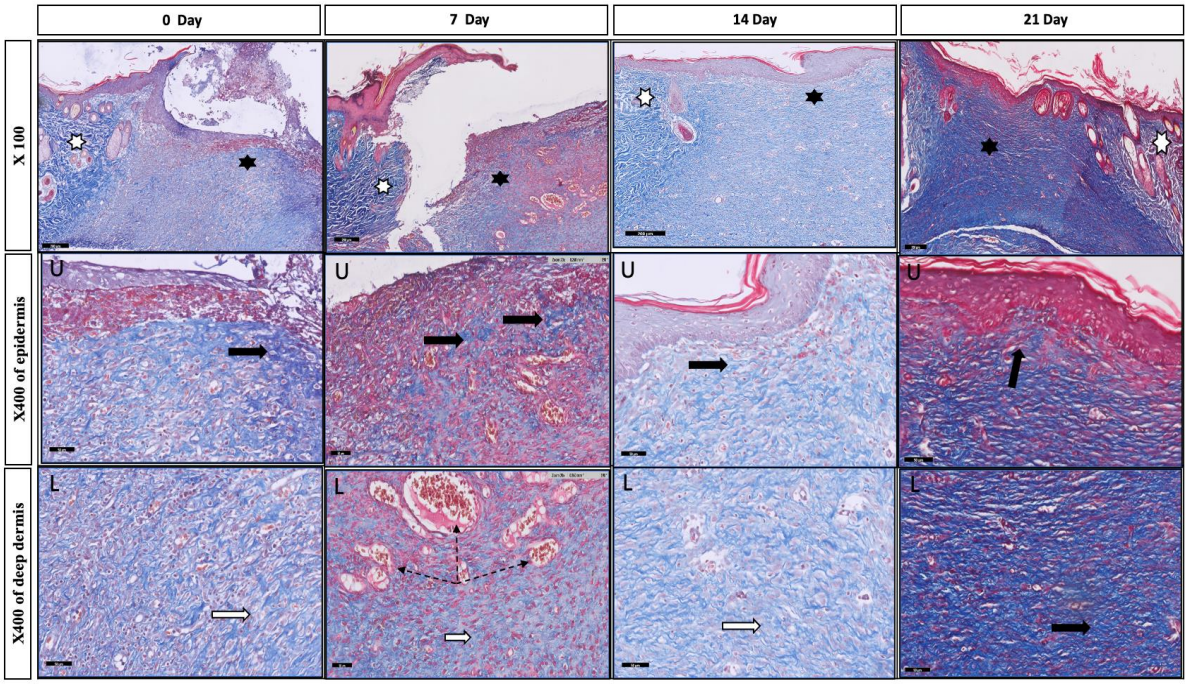

Fig. 11. Representative images of Masson Trichrome-stained histological sections of wounds from the control group (untreated) rats on days 0, 7, 14, and 21 post-wounding (magnifications x100, x400). Collagen in the wound area is marked with a black star, normal skin with a white star, a few mature collagen fibers with a black arrow, collagen in the deep dermis with a white arrow, and increased congested capillaries indicated by dotted arrows.

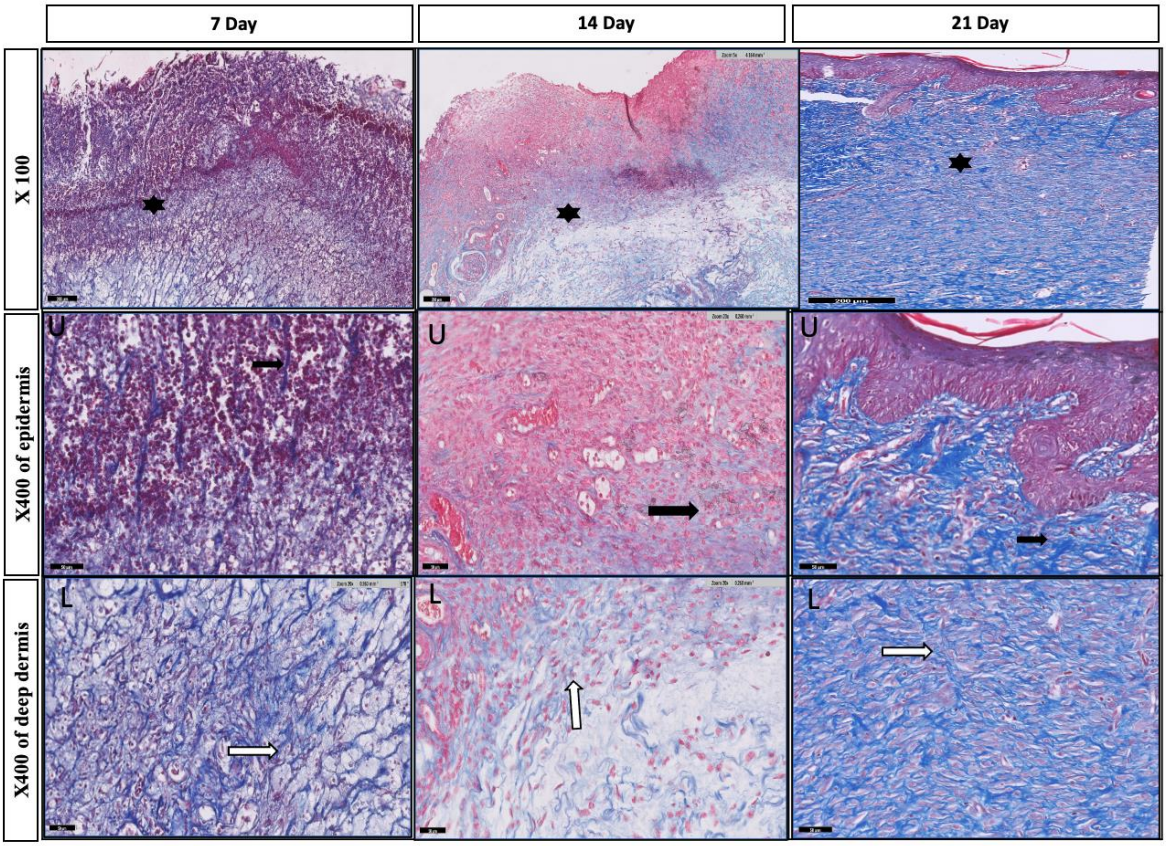

Fig. 12. Representative images of Masson Trichrome-stained histological sections of wounds from the diabetes group (untreated) rats on days 7, 14, and 21 post-wounding (magnifications x100, x400). Collagen in the wound area is indicated by a black star, a reduction in immature collagen fibers by a black arrow, and a small amount of stained immature fibers by a white arrow.

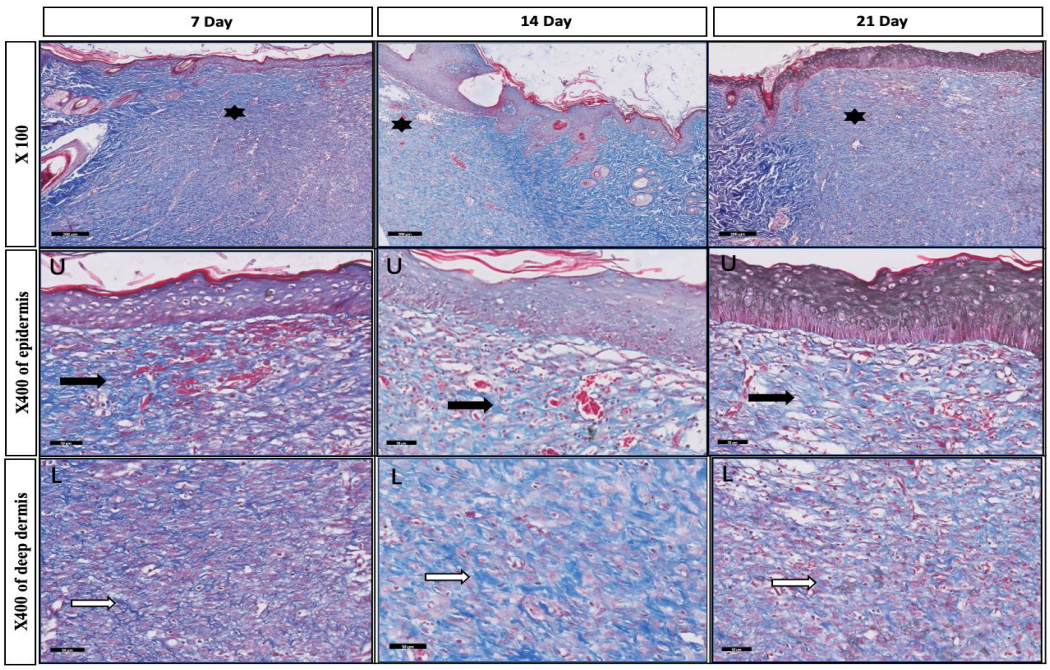

Fig.13: **Representative images of Masson Trichrome-stained histological wound sections from rats treated with pumpkin leaf nanoparticles (Cucurbita maxima) on days 7, 14, and 21 after wounding, at magnifications of x100 and x400. The images show collagen presence in the wound area (black star), the distribution of collagen within the deep dermis (white arrows), and immature collagen fibers (black arrows).**

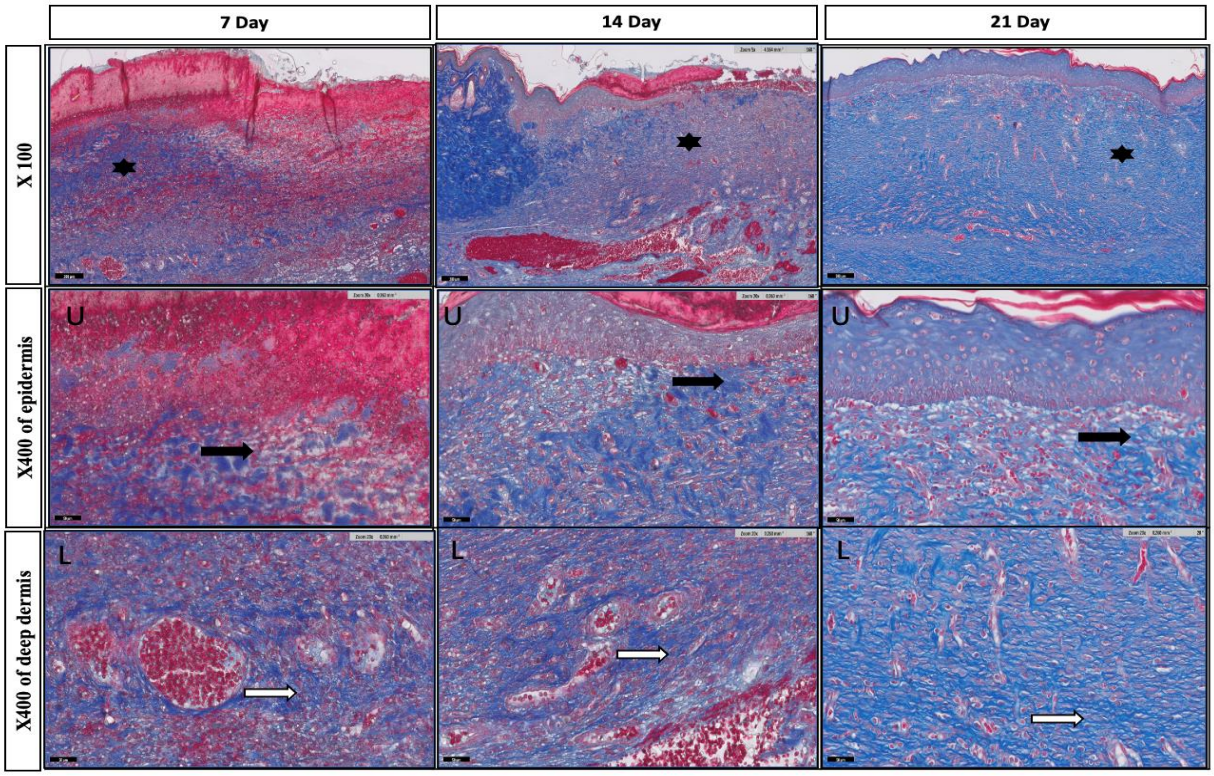

Fig. 14: **Representative images of Masson Trichrome-stained histological sections of wound tissue from diabetic rats treated with Silver Sulfadiazine, captured on days 7, 14, and 21 post-wounding (magnifications x100 and x400). The images highlight the presence of collagen in the wound area (marked by a black star), with a few mature collagen fibers (indicated by black arrows) and limited distribution of collagen in the deep dermis (denoted by white arrows).**

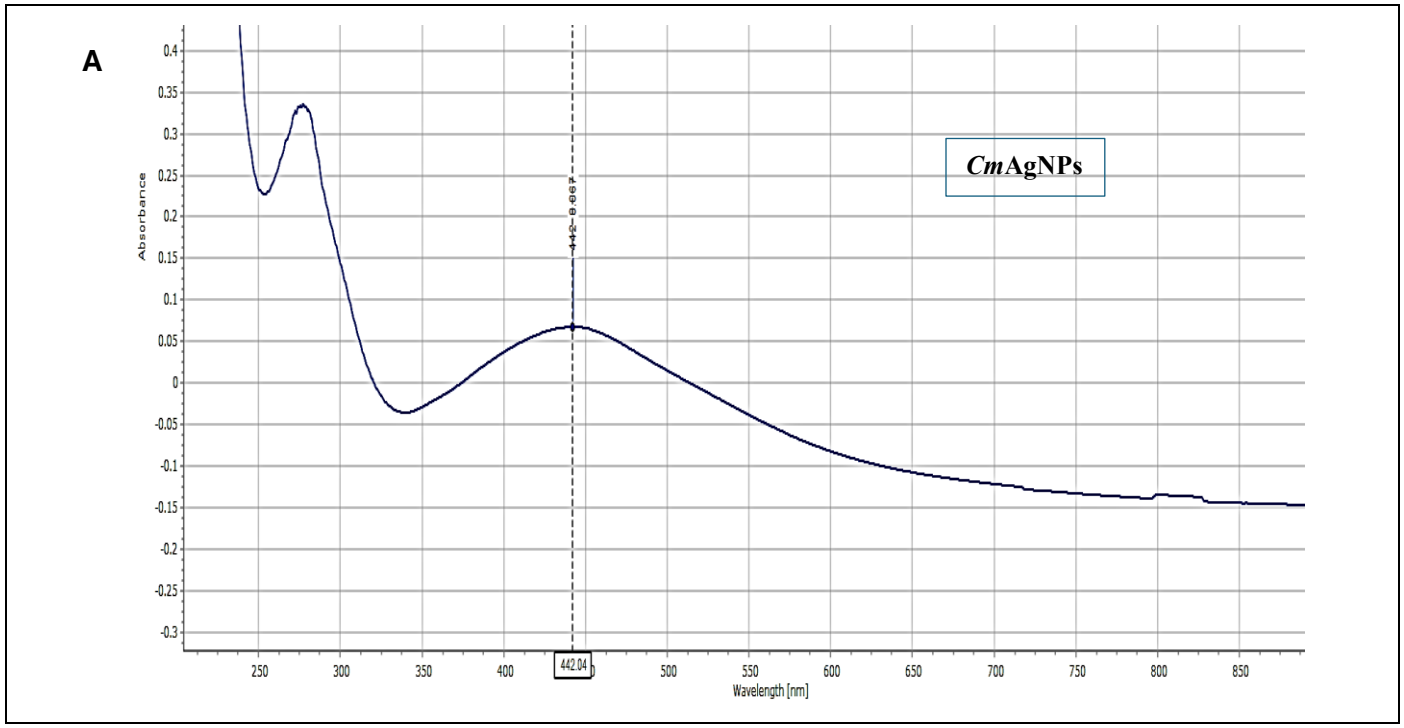

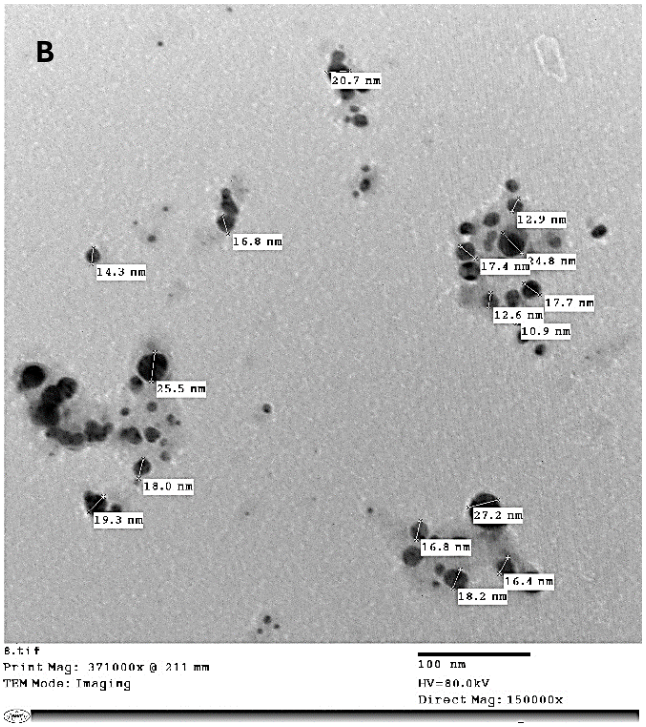

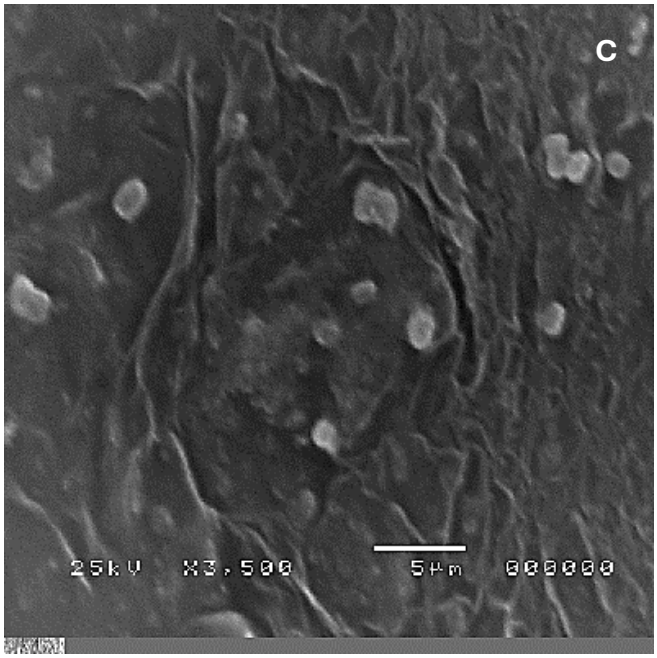

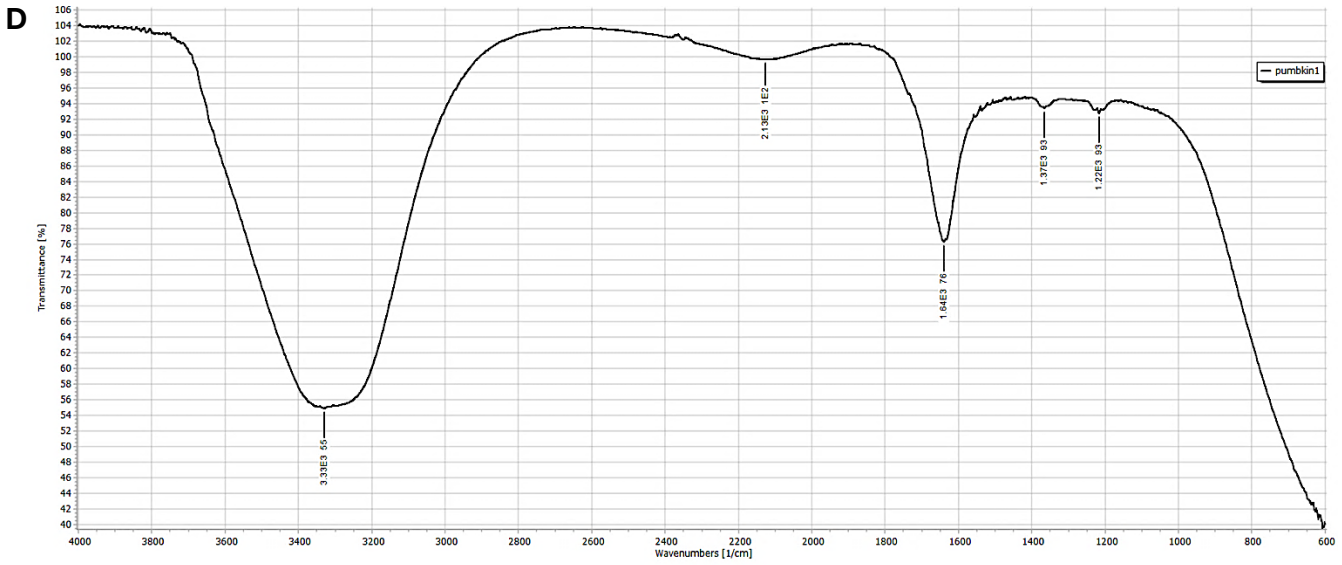

Figure S1: **(A) The UV-visible absorption spectrum of the biosynthesized *Cm*AgNPs, produced via the reduction of *Cucurbita maxima* extract solution after 60 minutes, shows a surface plasmon resonance peak at 442.04 nm, confirming nanoparticle formation. (B) TEM analysis reveals the nanoparticles as black spheres with an average size of 16.05 ± 0.02 nm. (C) SEM image of *Cm*AgNPs, captured at a magnification of 3,500x, displays white spherical beads predominantly ranging between 50 to 100 nm, suggesting a relatively uniform distribution and successful synthesis. (D) FTIR spectra of the biosynthesized *Cm*AgNPs show key absorption peaks around 3350 cm^{-1} (O-H stretching), 2920 cm^{-1} (C-H stretching), 1640 cm^{-1} (C=C stretching), 1450 cm^{-1} (C-H bending), and 1100 cm^{-1} (C-O stretching). These peaks indicate the presence of hydroxyl groups, alkanes, alkenes, and ether or ester functionalities, highlighting the involvement of organic compounds from plant extracts in the synthesis and stabilization of the silver nanoparticles.**

Discussion

Hemostasis, inflammation, proliferation, and remodeling are the four overlapping phases of wound healing [27]. In the inflammatory phase, infections and dead tissue are removed by the infiltration of polymorphonuclear leukocytes (PMNs) and mononuclear cells (MNs) [28].

Infection exacerbates impaired wound healing in individuals with diabetes and contributes significantly to morbidity and mortality on a global scale [29].

One example of a highly effective agent that inhibits biofilm formation is nanoparticles, which possess antimicrobial properties [30,31].

Diabetes patients have impaired wound healing because of a deficiency in the signaling of cells and chemicals necessary for the regular processes of wound healing, such as neovascularization, granulation tissue formation, epithelialization, and tissue remodeling. In healthy persons, the usual healing process proceeds to its full potential; in diabetics, however, it is frequently postponed or even completely disrupted [32].

In diabetic lesions, silver sulfadiazine and *Cm*AgNPs accelerated the WCR, promoting wound healing. As opposed to silver sulfadiazine lotion, *Cm*AgNPs has been demonstrated to be considerably superior. The observed phenomenon can be ascribed to preserving various phytochemicals, including antioxidants, linolenic acid, ascorbic acid, limonene, phytol, and linoleic acid. Furthermore, *Cm*AgNPs possess antimicrobial and anti-inflammatory properties that aid in bacterial eradication and promote wound tissue regeneration [33].

Silver nanoparticles synthesized from *Cucurbita maxima* (*Cm*AgNPs) were evaluated for their potential in promoting wound healing in a diabetic rat model. The formation of *Cm*AgNPs was confirmed by a distinct surface plasmon resonance (SPR) peak observed at approximately 442.04 nm. TEM analysis showed that the *Cm*AgNPs had an average diameter of 16.05 ± 0.02 nm. FTIR analysis identified functional groups derived from the pumpkin extract, which likely played a key role in the reduction and stabilization of the nanoparticles.

One crucial step in the healing process that leads to wound closure is the wound contraction rate, or WCR. As a result, in the macroscopic assessment of wound healing, visual appearances and measures of wound contraction become trustworthy parameters [34].

The Wound Closure Rate (WCR) was calculated to quantify the speed of wound healing. Previous research [35] [36] has identified WCR as a key indicator in the wound healing process. Studies have demonstrated that faster wound closure accelerates healing, while delayed closure can hinder recovery [37].

By accelerating the WCR, *Cm*AgNPs and silver sulfadiazine improved diabetic wound healing. But it was shown that *Cm*AgNPs was far superior to silver sulfadiazine cream. This may be explained by the antioxidants and other phytochemicals that were retained, including linolenic acid, ascorbic acid, limonene, phytol, linoleic acid, and phytol. Additionally, *Cm*AgNPs have antimicrobial and anti-inflammatory qualities that aid in the removal of bacteria while also promoting the growth of wound tissue [38].

The WCR of the NN group was consistently ($P<0.05$) higher than that of the DN group. Our results are corroborated by earlier research, which found that diabetic rats had a lower WCR than normal rats [35] [36].

The results indicate that on days 0, 7, and 14, the NN group exhibited slightly higher SOD activity in wound tissue compared to the other groups, although the difference was not statistically significant ($P>0.05$). This supports the hypothesis that diabetes mellitus (DM) reduces SOD levels in wound tissue [39]. *Cm*AgNPs had no significant effect on SOD levels.

DM with complication has lowest SOD and GSH activity but the malondialdehyde MDA level was found to be higher amongst studied groups indicating more reactive species generation to reduce the lipids due to oxidative stress [40]. DM has been shown to lower SOD levels in a variety of tissues, including skin [39] and retina [41] in diabetic animals.

As a result of their antioxidant properties, medicinal plants enhance the phase of proliferation and wound healing [42]. Therefore, removing O_2 and OH is probably one of the most effective defenses against diseases [43].

In the current study, it was found that *Cm*AgNPs gave a significant increase in GSH and SOD levels compared to another study. This finding aligns with a previous study [44], which demonstrated that the pumpkin extract inhibited lipid peroxidation and enhanced the activity of antioxidant enzymes, including glutathione peroxidase (GSH) and SOD.

Some studies have shown that pumpkin leaves are rich in antioxidants such as ascorbic acid and phenolics [45].

SOD plays a crucial role in preventing the formation of new free radicals and acts as the body's primary defense against O_2. The results clearly indicate that glutathione levels declined in the presence of diabetes, consistent with findings from previous studies. The reduction in SOD may be attributed to enzyme glycation or inactivation by H_2O_2, both of which have been associated with diabetes [46].

This may be due to the presence of high antioxidant (e.g. polyphenols) content in pumpkin leaves [45].

The topical application of CmAgNPs in this study resulted in a significant reduction in MDA levels and a marked increase in the antioxidant enzymes GPX and SOD in the skin [47].

Histological analysis revealed that CmAgNPs promoted the re-epithelialization process in the treated group. This suggests that CmAgNPs may play a role in activating dermal fibroblasts and keratinocytes, as well as enhancing collagen synthesis, which forms the foundation of the extracellular matrix. This matrix supports epithelialization during the healing phases and is considered a crucial step in wound healing [48].

In the contrary, the DN group's wound tissue displayed irregular collagen, inadequate epidermal development, and the presence of inflammatory cells, all of which could be linked to a delayed healing process. A prior study revealed the same results [49, 50]. Also, the silver sulfadiazine treatment group was showed no obvious epithelialization and incomplete regeneration of the epidermis and the dermis layer. These results suggest that *Cm*AgNPs has antimicrobial effects after a brief course of treatment. Studies have shown that pumpkin seed oils have therapeutic properties [33, 48].

In comparison to the DN and SSD groups, the histological examination of the wound tissue from the *Cm*AgNPs group revealed more newly formed blood vessels. The findings imply that *Cm*AgNPs might aid in the process of angiogenesis. Similar results were reported in another studies [33].

In this study, CmAgNPs proved to be more effective in treating wounds compared to silver sulfadiazine, which showed slower rates of wound contraction and reduced healing activity. This may be attributed to the delayed healing effects and cytotoxicity

of the ointment [51]. Silver sulfadiazine is primarily used as an antibacterial agent in wound treatment, owing to the actions of silver ions [52]. In comparison to the SSD and DN groups, the *Cm*AgNPs group displayed a greater collagen fiber content on days 14 and 21. The findings might bolster the claim that *Cm*AgNPs can stimulate the synthesis and deposition of collagen.

Nanoparticles synthesized from *Cucurbita maxima* extracts, specifically from the leaves, possess wound healing potential due to their influence on hydroxyproline levels in treated wound tissue. These levels increased during treatment periods, indicating that the extracts' activity may be related to the increased hydroxyproline (collagen substrate) influence on the early proliferation phase in treated wounds which was revealed by other study [53].

Extracellular matrix (ECM) is mostly composed of collagen, which plays an important role in wound healing. This process begins soon after a skin damage and lasts for several weeks [54]. It was discovered that the low collagen concentration in the DN group was comparable to the results of an earlier investigation [55].

Conclusions

Our findings suggest that nanoparticles synthesized from pumpkin leaf extracts (*Cm*AgNPs) enhance tissue healing and repair processes, likely due to their diverse phytochemical compositions. Unlike the slower wound regeneration seen with silver sulfadiazine, the therapeutic effects of *Cm*AgNPs include complete wound recovery, increased collagen deposition, and the restoration of normal skin appearance post-treatment. These results support the potential use of plant extracts as natural alternatives to conventional wound care. However, further research is needed to explore the role of different solvent extracts in the healing mechanisms for potential medical applications.

Acknowledgment

We would like to extend our thanks to Prof. Hayam Sami Abdelkader, Professor of Molecular Biology, Virus Research Department, Agricultural Research Center, Egypt, for her invaluable collaboration in the synthesis and characterization of biogenic nanoparticles, as well as her guidance, meticulous editing, and insightful revisions of the manuscript.

References

Farghaly Aly, U., Abou-Taleb, H. A., Abdullatif A. A., and Sameh Tolba, N. (2019). Formulation and evaluation of simvastatin polymeric nanoparticles loaded in hydrogel for optimum wound healing purpose. *Drug Des Devel Ther,* 13: 1567—1580.

Kant, V., Gopal, A., Pathak, N.N., Kumar, P., Tandan, S.K. and Kumar, D. (2014). Antioxidant and anti-inflammatory potential of curcumin accelerated the cutaneous wound healing in streptozotocin-induced diabetic rats. *Int. Immunopharmacol,* 20: 322–330.

Rafehi, H., El-Osta, A. and Karagiannis, T.C. (2011) Genetic and epigenetic events in diabetic wound healing. *Int Wound J,* 8 (1): 12–21.

Ram, M., Singh, V., Kumar, D., Kumawat, S., Gopalakrishnan, A., Lingaraju, M. C. and Kumar, D. (2014). Antioxidant potential of bilirubin-accelerated wound healing in streptozotocin-induced diabetic rats. *Naunyn-Schmiedeberg's Archives of Pharmacology,* 387(10): 955–961.

Majtan, J. (2011). Methylglyoxal—a potential risk factor of manuka honey in healing of diabetic ulcers. *Evidence-Based Complementary and Alternative Medicine, 2011,* 1.

Chellappan, D. K., Yenese, Y., Wei, C. C., and Gupta, G. (2017). Nanotechnology and Diabetic Wound Healing: A Review. *Endocr Metab Immune Disord Drug Targets,* 17 (2): 87-95.

Nikaein, D., Khosravi, A. R., Moosavi, Z., Shokri, H., Erfanmanesh, A., Ghorbani-Choboghlo, H., & Bagheri, H. (2014). Effect of honey as an immunomodulator against invasive aspergillosis in BALB/c mice. *Journal of Apicultural Research*, 53(1): 84–90.

Sharma, A., Sharma, A.K., Chand, T., Khardiya,M. and Yadav, K. C. (2013). Antidiabetic and Antihyperlipidemic Activity of *Cucurbita maxima Duchense* (Pumpkin) Seeds on Streptozotocin Induced Diabetic Rats. *Journal of Pharmacognosy and Phytochemistry,* 1(6): 108-116.

Tarameshloo, M., Norouzian, M., Zarein-Dolab, S., Dadpay, M., Mohsenifar, J., and Gazor, R. (2012). Aloe vera gel and thyroid hormone cream may improve wound healing in Wistar rats. *Department of Anatomy and Cell Biology*, 45(3): 170–177.

Lekshmi, P. N. C. J., Sowmia, N., Viveka, S., Brindha, J. R., and Jeeva, S. (2012). The inhibiting effect of Azadirachta indica against dental pathogens. *Asian J Plant Sci Res,* 2(1):6-10.

[**agi, S., and Ahmed, A. (2019).** Green production of AgNPs and their phytostimulatory impact. *Green Processing and Synthesis,* 8 (1):885-894.

FURMAN, B.L. (2015). Streptozotocin-induced diabetic models in mice and rats. *Curr Protoc Pharmacol,* 70: 41-20.

Eyarefe, O. D., Ologunagba, F. M., and Emikpe, B.O. (2014). Wound healing potential of natural honey in diabetic and non-diabetic wistar rats. *African Journal Biomedical Research,* 17(1):15-21

Hon Kwon, M.D. , Zeyu, Q., Hashimoto, M., Yamamoto, K. and Kimura, T. (2009). Effects of medicinal mushroom (*Sparassis crispa*) on wound healing in streptozotocin-induced diabetic rats. *The American Journal of Surgery,* 197: 503–509.

Shaik. R.A., Eid, B.G. (2022). Piceatannol Affects Gastric Ulcers Induced by Indomethacin: Association of Antioxidant, Anti-Inflammatory, and Angiogenesis Mechanisms in Rats. *Life (Basel, Switzerland),* 12(3).

Khan, M. A., Shahzadi, T., Malik, S. A., Shahid, M., Ismail, M., Zubair, M., and Iqbal, S. (2019). Pharmacognostic evaluation of turmeric (Curcuma longa) extracts in diabetic wound healing. *The Journal of Animal & Plant Sciences, 2*9(1): 68-74.

KUMAR, M.S., KIRUBANANDAN, S., SRIPRIYA, R., SEHGAL, P.K. (2008). Triphala promotes healing of infected full-thickness dermal wound. *J Surg Res,* 144: 94-101.

Guo, H.F., Ali R. M., Hamid, R. A., Zaini, A. A., Khaza'ai, H. (2017). A new model for studying deep partial-thickness burns in rats. *Int J Burns Trauma,* 7(6):107–14.

Karina, Samudra, M. F., Rosadi, I., Afini, I., Widyastuti,

T. and Sobariah, S., et al. (2019). Combination of the stromal vascular fraction and platelet-rich plasma accelerates the wound healing process: Pre-clinical study in a Sprague- Dawley rat model. *Stem Cell Investig,* 6:18.

Malkoc, M., Yaman, S. O., Imamoglu, Y., Imran, I., Kural, B. V., Mungan, S., Livaoglu, M., Yıldız, O., Kolaylı, S. and Oremb, A. (2019). Anti-inflammatory, antioxidant and wound-healing effects of mad honey in streptozotocin-induced diabetic rats. *Journal of Apicultural Research,* 59(4): 426-436

Goth, L. (1991). A simple method for determination of serum catalase activity and revision of reference range. *Clinica Chimica Acta,* 196(2–3): 143–151.

Sun, Y. I., Oberley, L. W., and Li, Y. (1988). A simple method for clinical assay of superoxide dismutase. *Clinical Chemistry,* 34(3): 497–500.

Uchiyama, M., and Mihara, M. (1978). Determination of malonaldehyde precursor in tissues by thiobarbituric acid test. *Analytical Biochemistry,* 86(1), 271–278.

Soliman, A. M., Lin, T. S., Ghafar, N. A., and Das, S. (2018). Virgin coconut oil and diabetic wound healing: histopathological and biochemical analysis. *European journal of anatomy*, 22 (2): 135-144.

Arkin, H. and Colton, R. R. (1963). Table for statisticians. *New York: Barnes& Noble.*

Hill, M. O. (1973). Reciprocal averaging: an eigenvector method of ordination. *J Eco,* 61:237- 249.

Stone, Ii. R. , Natesan, S., Kowalczewsk, I C. J., Mangum, L. H., Clay, N. E., Clohessy, R. M. (2018). et al. Advancements in Regenerative Strategies Through the Continuum of Burn Care. *Frontiers in pharmacology,* 9:672.

Orihuela, R., McPherson, C. A., Harry G. J. (2016). Microglial M1/M2 polarization and metabolic states. *British journal of pharmacology,* 173 (4):649–65.

Falanga, V. (2005). "Wound healing and its impairment in the diabetic foot," *Lancet,* 366 (9498): 1736-1743.

Ramasamy, M., Lee, J. (2016). Recent nanotechnology approaches for prevention and treatment of biofilm-associated infections on medical devices. *Biomed Res Int,* 1851242.

Simões, D., Miguel, S. P., Ribeiro, M. P., Coutinho, P., Mendonça, A. G., Correia, I. J., (2018). Recent advances on antimicrobial wound dressing: a review. *Eur. J. Pharm. Biopharm,* 127:130-141.

D. G. Greenhalgh, D. G. (2003). Wound healing and diabetes mellitus. *Clinics in Plastic Surgery,* 30 (1): 37-45.

Thamer, S. J., Ibrahim, M. K. and Alnema, K. S. (2021). Evaluation of the healing activity of *Cucurbita spp.* leaf and seed extracts on experimental thermal burns. *Karbala International Journal of Modern Science,* 7(4): 10

Gal, P., Kilik, R., Mokry, M. et al. (2008). Simple method of open skin wound healing model in corticosteroid-treated and diabetic rats: standardization of semi-quantitative and quantitative histological assessments. *Veterinarni Medicina,* 53 (12): 652-659

Qiu, Z., Kwon, A. H. and Kamiyama, Y. (2007). Effects of plasma fibronectin on the healing of full-thickness skin wounds in streptozotocin- induced diabetic rats. *J Surg Res,* 138:64-70

Teoh SL, Latiff A.A. and Das, S. (2009). The effect of topical extract of Momordica charantia (bitter gourd) on wound healing in nondiabetic rats and in rats with diabetes induced by streptozotocin. *Clin Exp Dermatol,* 34 (7): 815-22

Jeffcoate, W. J., Price, P., Harding, K. G. (2004). Wound healing and treatments for people with diabetic foot ulcers. *Diabetes Metab Res Rev,* 20: 78-89.

Thamer, S. J., Ibrahim, M. K. and Alnema, K. S. (2021). Evaluation of the healing activity of Cucurbita spp. leaf and seed extracts on experimental thermal burns. *Karbala International Journal of Modern Science,* 7(4): 10

Jankovic, A., Ferreri, C., Filipovic, M., Ivanovicburmazovic, I., Stancic, A., Otasevic,V., Korac,A., Buzadadzic, B., Korac, B. (2016). Targeting the superoxide/nitric oxide ratio by L-arginine and SOD mimic in diabetic rat skin. *Free Radic Res,* 50: 51-63.

Giacco, F., Brownlee, M., SchmidtAnn, M. (2010). Oxidative Stress and Diabetic Complications. *Circ.Res.,*107: 1058-1070.

Kowluru, R. A., Atasi, L., HO, Y. S. (2006). Role of mitochondrial superoxide dismutase in the development of diabetic retinopathy. *Invest Ophthalmol Vis Sci,* 47: 1594-1599.

Süntar, I., Akkol, E. K., Nahar, L., and Sarker, S. D. (2012). Wound healing and antioxidant properties: do they coexist in plants? *Free Radicals and Antioxidants,* 2(2): 1-7.

Sankaranarayanan, C. and Pari, L. (2011). Thymoquinone ameliorates chemical induced oxidative stress and β-cell damage in experimental hyperglycemic rats. *Chemico-Biological Interactions,* 90(2), pp. 148-154.

Murugan, P. and Pari, L. (2006). Antioxidant effect of tetrahydrocurcumin in streptozotocin–nicotinamide induced diabetic rats. Life Sciences, 79(18), pp. 1720-1728.

Oboh, G. (2005). Hepatoprotective property of ethanolic and aqueous extracts of fluted pumpkin (Telfairia occidentalis) leaves against garlic-induced oxidative stress. *J. Med. Food,* 8(4):560-563.

Sozmen, E.Y., Sozmen, B., Delen, Y. and Onat, T. (2001). Catalase/superoxide dismutase (SOD) and catalase/paraoxonase (PON) ratios may implicate poor glycemic control. *Archives of Medical Research,* 32(4), pp. 283-287.

Almohaimeed, H. M., Al-Zahrani, M. H., Almuhayawi, M. S., Algaidi, S. A., Batawi, A. H. et al. (2022). Accelerating Effect of *Cucurbita pepo* L. Fruit Extract on Excisional Wound Healing in Depressed Rats Is Mediated through Its Anti-Inflammatory and Antioxidant Effects. *Nutrients,* 14: 33-36.

Bardaa, S., Ben Halima, N., Aloui, F., Ben Mansour, R., Jabeur, H., Bouaziz, M., Sahnoun, Z. (2016). Oil from pumpkin (*Cucurbita pepo* L.) seeds: Evaluation of its functional properties on wound healing in rats. *Lipids Health Dis,* 15: 73.

Qiu, Z., Kwon, A. H. and Kamiyama, Y. (2006). Effects of plasma fibronectin on the healing of full-thickness skin wounds in streptozotocin- induced diabetic rats. *J Surg Res,* 138:64-70

Teoh SL, Latiff A.A. and Das, S. (2009). The effect of topical extract of Momordica charantia (bitter gourd) on wound healing in nondiabetic rats and in rats with diabetes induced by streptozotocin. *Clin Exp Dermatol,* 34 (7): 815-22

Rashaan, Z., Krijnen, P., Klamer, R., Schipper, I. and Dekkers, O. (2014). Non silver treatment versus silver sulfadiazine in treatment of partial thickness burn wounds in children: a systematic review and meta-analysis. *Wound Repair Regen,* 22(4):473-82.

Espiritu, A., Lao, S. and Guerrero, J. (2016). Burn wound healing potential of Bixa orellana Linn [Bixaceae] leaf extracts on albino mice, *J. Med. Plants Stud,* 4(1): 84-87

Priya, K., Arumugam, G., Rathinam, B., Wells, A., Babu, M. (2004). Celosia argentea Linn. Leaf extract improves wound healing in a rat burn wound model. *Wound Repair Regen,* (2): 618-625.

SHOSHAN, S. (1981). Wound healing. *Int Rev Connect Tissue Res,* 9: 1-26.

DOGAN, E., YANMAZ, L., GEDIKLI, S., ERSOZ, U., OKUMUS, Z. (2017). The effect of pycnogenol on wound healing in diabetic rats. *Ostomy Wound Manage,* 63: 41-47.